



Empirical attribution of a drying Himalayan river through remote sensing and secondary data

Gopal Penny^{1,2}, Zubair A. Dar³, and Marc F. Müller^{1,2}

¹Environmental Change Initiative, University of Notre Dame, Indiana, USA

²Civil and Environmental Engineering and Earth Sciences, University of Notre Dame, Indiana, USA

³Energy and Resources Group, University of California, Berkeley, California, USA

Correspondence: Gopal Penny (gopalpenny@gmail.com)

Abstract. Streamflow regimes are rapidly changing in many regions of the world. The ability to attribute these changes to specific hydrological processes and their underlying climatic and anthropogenic drivers is essential to formulate effective water policy. Traditional approaches to hydrologic attribution rely on the ability to infer hydrological processes through the development of catchment-scale hydrological models. However, such approaches are challenging to implement in practice. In particular, models have difficulty capturing hydrological regime shifts, where changes in the dominant hydrological processes alters the relationship among hydrological fluxes. Additionally, observational uncertainties might preclude closure of the catchment-scale water balance, which is a pre-requisite for most catchment-scale hydrological models. Here we present an alternative approach to hydrological attribution that leverages the method of multiple hypotheses. We generate and empirically evaluate a series of alternative and complementary hypotheses that pertain to hydrological change. These hypotheses concern distinct components of the water balance and are evaluated independently. This process allows a holistic understanding of watershed-scale processes to be developed, even if the catchment-scale water balance remains open. We apply the approach to understand changes in the Upper Jhelum river, an important tributary headwaters of the Indus basin, where streamflow has declined dramatically since 2000 and has yet to be adequately attributed to its corresponding drivers. Using remote sensing and secondary data collected from the watershed, we explore changes in climate, surface water, and groundwater. The evidence reveals that climate, rather than land use, had a considerably stronger influence on reductions in streamflow, both through reduced precipitation and increased evapotranspiration.

1 Introduction

Water resources are changing throughout the world under anthropogenic pressures including climate change, land use change, and changes in water management (Vörösmarty et al., 2004; Milly et al., 2008; Ceola et al., 2019). These drivers pose challenges for water policy by increasing climatic variability (Smirnov et al., 2016), exacerbating water-scarcity (Srinivasan et al., 2017), and reducing our ability to predict hydrological variables (Ehret et al., 2014). In arid and semi-arid regions, these concerns are particularly alarming given the concurrent challenges of increasing hydrological uncertainty and competition for scarce water resources (Flörke et al., 2018; Aeschbach-Hertig and Gleeson, 2012). In many such regions, mitigation and adaptation strategies are urgently needed but require accurate understanding of the underlying drivers of change (Thompson et al.,



25 2013; Penny et al., 2020a). In order to address the management challenges of mitigation and adaptation, observed changes in
the hydrological processes must be correctly attributed to corresponding hydrological drivers. However, despite advances in
computational power, large-scale hydrological models, and the satellite-driven big data revolution (Kitchin, 2014; Sheffield
et al., 2018), the relative importance of various hydrological drivers in many watersheds remain unknown. Even the basic task
of accurately measuring the water balance may create considerable obstacles (Kampf et al., 2020). Changes in the water bal-
30 ance may go unnoticed and attributing the drivers of change creates additional scientific obstacles (Wine and Davison, 2019).
Water policy will therefore benefit from approaches to attribution that address hydrological science questions at scales pertinent
to management (Müller and Levy, 2019; Penny et al., 2020b).

Attribution seeks to explain hydrological processes by demonstrating a causal relationship between observed outcomes
and their associated drivers. Hydrological attribution has been approached through a variety of methods including hydrological
35 simulation (Liu et al., 2019), fingerprinting (Viglione et al., 2016), ecohydrological signatures (Tomer and Schilling, 2009), and
Budyko-based models (Ning et al., 2018). In each of these methods, causal relationships are incorporated into models which are
then tested against hydrological records (Dey and Mishra, 2017). Goodness-of-fit and other model evaluation metrics influence
which models are given more credibility (Müller and Thompson, 2019) and which models are, in turn, used to identify the
causal processes in the attribution. This approach is referred to as predictive inference (Ferraro et al., 2019), which mirrors the
40 widely recognized approach of “top-down” hydrological modeling. A defining feature of both predictive inference and top-
down hydrological modeling is that hypotheses are incorporated into models and tested against observations (Savenije, 2009).
Predictive inference is appealing given the flexibility of the approach to a range of hydrological systems and because it can be
easily adapted to generate counterfactual scenarios to assess the effects of specific drivers. The major challenge of using such
top-down approaches for attribution is the difficulty in validating hydrological processes within the model. These difficulties
45 can arise due to equifinality (cannot distinguish drivers by considering outcomes only, Beven, 2006), nonlinearity (drivers are
not linearly separable, Sivapalan, 2006), hydrological regime shifts (Foufoula-Georgiou et al., 2015; Gober et al., 2017), or
lack of appropriate data (cannot test hypotheses pertaining to specific processes, Sheffield et al., 2018). Calibrated models
have particular difficulty with hydrological regime shifts, where the underlying mechanisms of streamflow generation change
yet these change cannot be directly observed (Savenije, 2009). Additionally, limited data is particularly problematic given the
50 common difficulties in closing the water balance at both large (e.g., watershed) and small (e.g., hillslope or plot) scales (Kampf
and Burges, 2010; Safeeq et al., 2021).

Here, we advance an alternative, “bottom-up”, approach to attribution, wherein several plausible hypotheses are generated
and each is evaluated *separately*. The approach is grounded in the method of multiple working hypotheses (Chamberlin, 1965)
and has two key benefits. First, the approach does not rely on constructing and calibrating a fully integrated catchment-scale
55 hydrological model. The approach only relies on the specific sets of empirical observations that are necessary to individually
test each hypothesis. As such, it is particularly helpful in data-scarce catchments, where limited hydrological records preclude
complete characterization of the water balance and data collection may be difficult. Relatedly, the bottom-up approach allows us
to explicitly account for uncertainties in hydrological fluxes or issues with data integrity. These issues might cause some (though
not all) hypotheses to be inconclusively evaluated. This contrasts with the top-down approach, where integrity issues with some



60 of the data might cause the whole analysis to be inconclusive, or worse, be concealed within the model calibration process (e.g.,
due to equifinality issues). Second, the approach mitigates against conceptual biases in which certain hypotheses are favored
based on preconceived notions of change (Railsback et al., 1990). By employing separate analyses for each hypothesis, we
construct a process-based narrative of attribution in which each analysis comprises part of the whole and serves to corroborate
or contradict other analyses. Indeed, the method of multiple hypotheses advocates broader understanding of the whole over
65 in-depth understanding of individual components. By favoring breadth over depth we seek to develop a coherent and holistic
narrative of change.

Although initially proposed in 1890 (and later republished as Chamberlin, 1965), few studies have applied the method of
multiple hypotheses towards hydrological attribution. Harrigan et al. (2014) used the method of multiple hypotheses to demon-
strate the combined effect of changing precipitation and catchment drainage in producing greater streamflow. Additionally,
70 Srinivasan et al. (2015) sought to attribute hydrological change in a drying river by generating (and subsequently testing) a
set of hypotheses based on stakeholder knowledge. Here, we apply the bottom-up approach and employ the water balance as
a guiding framework to generate hypotheses regarding hydrological processes while using stakeholder knowledge to provide
additional context with respect to water management. We note that this differs from bottom-up hydrological modeling, which
seeks to aggregate catchment-scale hydrological processes by simulating physical mechanisms at small scales, and has been
75 criticized for taking a reductionist approach to catchment scale processes (Sivapalan et al., 2003; Savenije, 2009). We avoid
reductionism by focusing on catchment-scale processes and linking finding from multiple hypotheses to develop a coherent
understanding.

Our empirical approach to hydrological attribution by leverages remote sensing information to complement gaps in observa-
tional data. We focus on the Upper Jhelum watershed which serves as one of the main headwaters of the Indus river and where
80 changes in hydrology (Wetlands International South Asia, 2007) have produced considerably less streamflow since the year
2000. The Upper Jhelum provides critical ecosystem services and water supply in the Kashmir Valley and irrigation down-
stream in Pakistan (Romshoo, 2012). Water security in both countries is threatened by climate change, land use change, and
competition for scarce water resources (Akhter, 2017). Given the importance of this river, scientific understanding of changing
hydrological processes is essential to support effective domestic and transboundary water management. Considerable hydrolog-
85 ical research at the basin scale has focused on streamflow forecasting (e.g., Mahmood and Jia, 2016; Badar et al., 2013), along
with empirical work characterizing streamflow in tributaries and the hinterlands (Jeelani, 2008; Jeelani et al., 2013; Romshoo
et al., 2015). As yet, little empirical research has addressed changes in the main stem of the Upper Jhelum. Political turmoil in
the basin poses challenges for data collection and research, meaning that a combination of remote sensing and secondary data
analysis currently represent an important opportunity for understanding hydrological change. This research therefore serves
90 the dual purposes of advancing a new approach to hydrological attribution and providing a scientific foundation that supports
regional water management. Furthermore, many of the scientific and management challenges in the Upper Jhelum are common
in arid- and semi-arid regions and low- and middle- income countries, including a limited ability to collect data (Sheffield et al.,
2018), strong reliance on water resources for economic productivity by a large portion of the population (Alexandratos, 2005),
and inequities in water access and water scarcity that pose considerable risks to rural livelihoods (Hussain and Hanjra, 2003).



95 Observational field studies have served as the foundation for understanding hydrological processes because they must con-
tend with hydrological complexity. Field studies have been used extensively to understand causal relationships at a range of
spatial scales. However, field studies are limited by resource constraints (time and money), inaccessibility of field locations, or
inability to observe historical processes *ex-post*. The latter challenge can be addressed in some cases by using space-for-time
substitution or water infrastructure to generate historical data (Penny et al., 2020b). Yet considerable challenges remain, espe-
100 cially in human-impacted catchments, due to the difficulty in capturing spatial complexity and ruling out potential alternative
drivers of change (Srinivasan et al., 2015).

In that context, remote sensing offers tremendous potential to overcome both major limitations of field experimentation in
terms of capturing spatial heterogeneity and generating observational datasets *after* hydrological changes occur and are de-
tected (e.g., Valentín and Müller, 2020). The increasing availability of remote sensing products has provided satellite estimates
105 of precipitation, evapotranspiration, and changes in water storage including surface water, soil moisture, and groundwater
(Montanari and Sideris, 2018). As satellite missions become operational, the ability to retrospectively generate hydrological
datasets grows to encompass the time period extending back to the satellite launch. However, satellites are currently unable
to directly monitor key components of the water balance (e.g., streamflow) or are limited in terms of resolution or accuracy.
For instance, precipitation estimates must be calibrated to gauged data and contain considerable uncertainty, particularly in
110 mountainous regions because the relationship between cloud top temperature and rainfall intensity is altered for orographic
effects (Müller and Thompson, 2013). Catchment-scale groundwater storage is particularly challenging to monitor. Radar sen-
sors (e.g., the Soil Moisture Active Passive mission) can monitor the dielectric properties of soils (associated with their water
content), but only up to depths of the order of 10^{-1} m (Chan et al., 2016). Interferometric synthetic aperture radars (InSAR)
can measure soil subsidence but requires substantial ancillary data to relate it to groundwater depletion (Levy et al., 2020).
115 Large scale changes in groundwater storage can be detected by monitoring the near-surface gravity field of Earth (i.e., through
the Gravity Recovery and Climate Experiment, or GRACE mission), but require a spatial averaging on the scale of 10^5 m
(Long et al., 2015). More fundamentally, most relevant satellites were launched circa 2000, providing a record over the last two
decades. This precludes analyses that extend into the 1990s, which is often necessary to establish a “pre-change” baseline. The
Landsat record provides coverage extending back to 1972, but many images prior to Landsat 7 (launched in 1999) are missing
120 from the publicly available USGS record, especially for regions outside the U.S. Despite these limitations, remote sensing
provides unique opportunities to attribute hydrological change in data-scarce regions (Müller et al., 2016; Penny et al., 2018).
This study demonstrates this potential in the context of a bottom-up attribution approach based on the method of multiple
hypotheses.

We first present an overview of the hydrogeophysical characteristics of the upper Jhelum and its change in flow regime
125 (Sect. 2). We then construct multiple hypotheses to explain the change in flow regime, considering possible changes in the
water balance due to changing climate, land use, and water storage (Sect. 3). For each of the hypotheses, we provide a detailed
description of the datasets (in Sect. 3) and present the results (Sect. 4). We then synthesize these results to construct a plausible
narrative of hydrological change in the catchment (Sect. 5), and conclude by discussing the potential for bottom-up attribution
and remote sensing to support understanding of hydrological change in data-scarce regions (Sect. 6).



130 2 Study site

2.1 Catchment layout

The upper Jhelum river serves as one of the six main tributaries of the Indus river (Fig. 1a), supporting residents in both India and Pakistan. The watershed covers approximately 13,000 km² and is bounded by the Himalayan range to the northeast and Pir Panjal range to the southwest, both of which drain into the Kashmir valley. The river flows east to west along the
135 Kashmir valley, passing through Wular lake before discharging at the outlet (Fig. 1b). The valley rests upon a layer of alluvial sediment which partially overlays a layer of glacial till, the combination of which extends nearly 1 km into the subsurface (Dar et al., 2014). Both mountain ranges on either side consist of limestone Karst formations, and streamflow is supported both by groundwater recharge in the valley and karst springs emerging from mountainsides (Jeelani, 2008).

The valley receives an average annual precipitation of 700–1250 mm per year, depending on elevation. Precipitation is
140 dominated by Mediterranean westerlies in the spring (March–May) and the Indian monsoon in the summer (June–September) (Zaz et al., 2019). Average valley temperatures range from 8°C in January to 29°C in August. Higher elevations remain below freezing in winter and streamflow receives a boost from snow melt as temperatures warm throughout the spring.

The main stem of the upper Jhelum is intercepted by Wular lake (Fig. 1d) between gauges (iii) and (iv). A number of other, smaller lakes intersect tributaries within the watershed and seasonally inundated wetlands occupy much of the center of the
145 valley (Fig. 1e). Agricultural land comprises the majority of the valley and supports rice paddy, maize, and wheat, as well as noticeably increasing fruit orchards (DES, 2015).

2.2 Declining streamflow

Streamflow in the main stem of the Upper Jhelum has declined over time. In particular, annual streamflow timeseries reveal a dramatic decline around the year 2000 (Fig. 1c). Average annual streamflow at the watershed outlet (Fig. 1b, gauge v) during
150 the 2000–2013 period (419 mm y⁻¹) reduced by 50% compared to the 1984–1999 period (852 mm y⁻¹), and by 27% compared to the 1944–1983 baseline (670 mm y⁻¹).

In addition to the above metrics for annual streamflow at the watershed outlet, streamflow observations were obtained from the The Department of Irrigation and Flood Control for Jammu and Kashmir at four additional stations (Fig. 1b) for the period 1955–2013. Standard data integrity checks (Searcy and Hardison, 1960) and flow separation (Nathan and McMahon, 1990)
155 procedures were applied to ensure temporal and spatial consistency (see Supplementary Information). We used these data in our evaluation of hypotheses, as described below.

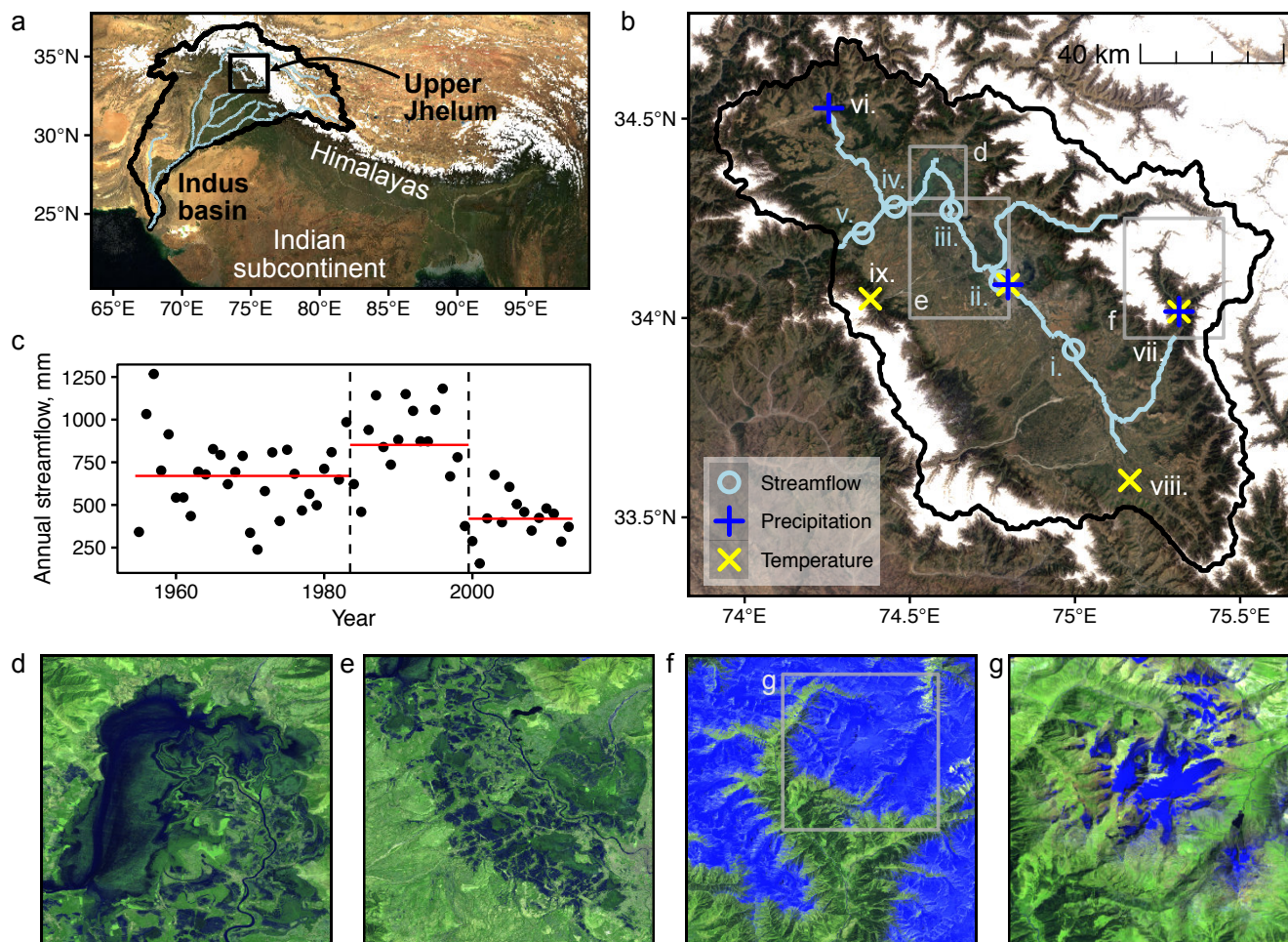


Figure 1. Study site and hydrological change. (a) Himalayan water towers including the Indus basin and location of the Upper Jhelum. (b) Upper Jhelum watershed including locations of streamflow records (gauges i–v), climate records (stations ii and vi–ix), and bounding boxes for (d–f). (c) Annual streamflow normalized by catchment area, with long-term averages for the periods 1955–1983 (670 mm, no climate data), 1984–1999 (852 mm, pre-2000 with climate data), and 2000–2013 (419 mm, post-2000). The remaining panels highlight water storage within the Upper Jhelum including (d) Wular lake, (e) valley inundation, (f) snow pack in May, and (g) Kolahoi glacier in August. In these images (d–g), Landsat bands swir2–swir1–red are mapped to red–green–blue, so that water and snow are clearly visible as dark and blue pixels, respectively. MODIS imagery in (a) (Vermote, 2015) and Landsat composite imagery in (b, d–g) from U.S. Geological Survey were prepared and downloaded using © Google Earth Engine (Gorelick et al., 2017).

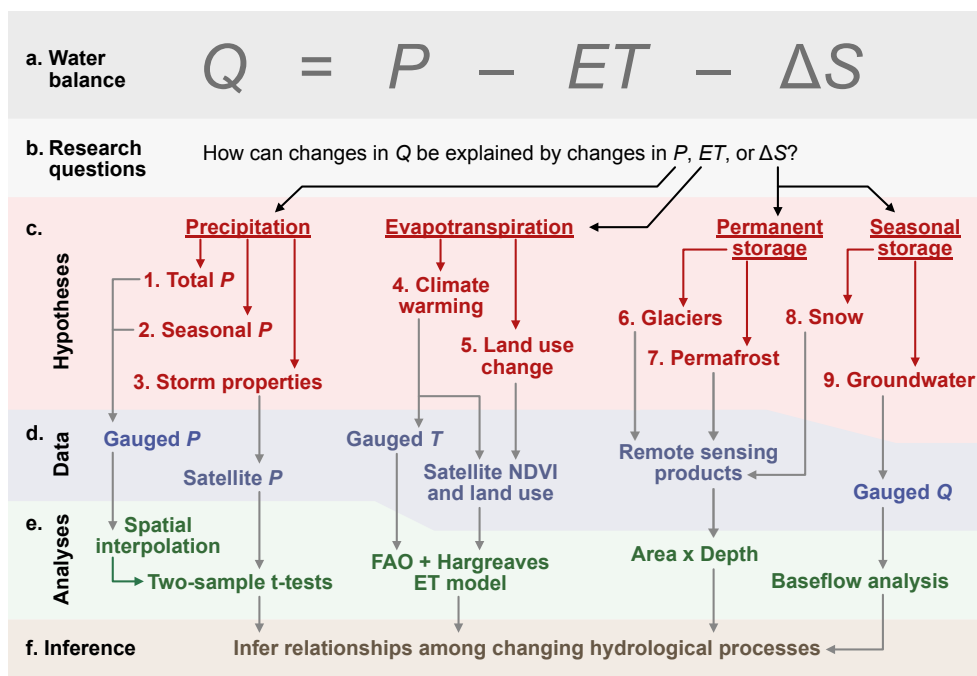


Figure 2. Hypothesis generation and evaluation. We develop a general empirical approach to attribution that (a) utilizes the water balance to (b) generate overarching research questions and (c) construct multiple hypotheses. The hypotheses are addressed (d) using remote sensing and *in situ* secondary data and (e) by applying empirical analyses, the results of which are (f) used to infer relationships regarding changing hydrological processes. We implement this approach in the Upper Jhelum watershed by defining the long-term water balance in terms of streamflow (Q), precipitation (P), evapotranspiration (ET), and changes in catchment water storage (ΔS). Specific research questions (red), data (blue), and analyses (green) focus on the detection and characterization of changing water balance fluxes in the Upper Jhelum. The inference step is contingent on understanding *how* each flux has changed and provides a deeper understanding of watershed hydrological processes.

3 Methods

3.1 Implementing the method of multiple hypotheses

We use the water balance as a guiding framework to attribute the decrease in Jhelum streamflow. In particular, it serves as a conceptual tool to build alternative hypotheses regarding changes in each of the water balance fluxes that could explain the observed reduction in streamflow (Fig. 2). Testing these hypotheses individually allows us to build understanding about the different pathways of hydrologic change throughout the catchment. Importantly, this approach does not rely on the predictive ability of an aggregate hydrological model, where calibration would depend upon on specific information that is not necessarily available. The multiple hypotheses are developed for each component of the water balance in the following paragraphs, along with approaches and datasets (also see Fig. 2, Table 1) to evaluate these hypotheses.



Table 1. Datasets used in analyses.

Dataset	Type	Source	Time period	Recurrence
Streamflow	Gauged	The Department of Irrigation and Flood Control (J&K Govt)	1955–2013	Daily–monthly
Precipitation	Station	Indian Meteorological Department (Srinagar)	1984–2013	Monthly
Temperature	Station	Indian Meteorological Department (Srinagar)	1984–2013	Monthly
Precipitation	Satellite	PERSIANN	1984–2013	Daily
Evapotranspiration	Satellite	MODIS ET Product	2000–2013	8-daily
Land use	Satellite	MODIS Land cover Product	2001, 2010	Annual
Snow and water extent analyses	Satellite	Landsat Missions 5, 7, 8	1989–2013	Varies

3.2 Precipitation

3.2.1 Hypotheses

Changes in precipitation (P) could occur through different mechanisms that would have distinct impacts on streamflow. For instance, a reduction in precipitation would decrease the water balance inputs and reduce the water available to generate streamflow. Alternatively, an increase in storm frequency and reduction in average storm size could produce an increase in vadose zone water storage, greater evapotranspiration (ET), and reduced streamflow (Zhao et al., 2019). We therefore pose the following hypotheses:

- Hypothesis 1: Changing climate led to a reduction of annual precipitation.
- Hypothesis 2: Changing climate led to a change in rainfall seasonality.

The first hypothesis represents a direct reduction in the water input to the catchment that would generate a reduction in streamflow. The second hypotheses represents a shift in the availability of water throughout the year. Such a shift in precipitation from a season with low ET to high ET could decrease average streamflow.

- Hypothesis 3: Changing climate led to greater storm frequency.

A reduction in storm size would reduce the “fast” component of streamflow (i.e., quickflow, McCaig, 1983) and combined with an increase in storm frequency the fraction of rain that is captured within the vadose zone would increase, leading to greater bare soil evaporation and plant water use (Zhao et al., 2019). These changes would reduce quickflow and groundwater recharge, and thus ultimately reduce annual streamflow volume.



3.2.2 Data sources

To address these hypotheses, monthly precipitation data were obtained from the Indian Meteorological Department (IMD, 185 Srinagar) for the period 1984–2013 at Srinagar, Kupwara, and Pahalgam stations (stations ii, vi, and vii in Fig. 1b). We interpolated monthly precipitation to the watershed scale using Thiessen polygons, which we found were able to close the water balance better than less parsimonious approaches that account for elevation gradients (see Sect. S2, Fig. S3).

The monthly frequency of the IMD precipitation dataset precluded analysis of storm recurrence. Therefore, we utilized daily precipitation records from the gridded PERSIANN Climate Data Record (CDR, Ashouri et al., 2015). The purpose of 190 PERSIANN CDR is to provide consistent precipitation data for long-term climate analysis dating back to 1984 at 0.25 degree resolution. We used PERSIANN data as an indication of temporal variation in the distribution of storm size and frequency. In particular, we counted the number of storms each year in each pixel to see if storm recurrence had changed.

3.3 Evapotranspiration

3.3.1 Hypotheses

195 Evapotranspiration (ET) affects streamflow by reducing the volume of water stored in the vadose zone that could have otherwise produced streamflow. A reduction in streamflow could therefore be generated by an increase in ET, either through changes in potential evapotranspiration or vegetation properties and land use. We therefore include the following hypotheses:

- Hypothesis 4: Climate change and warmer air temperatures led to greater evapotranspiration.
- Hypothesis 5: Land use change toward water-intensive crops led to greater evapotranspiration.

200 Both hypotheses are grounded in observed, ongoing changes within the watershed. Temperatures have been warming (Zaz et al., 2019) and there has been a notable shift towards orchard plantations in portions of the valley (Romshoo and Rashid, 2014), which may use more water than traditional crops due to a longer growing season (Allen et al., 1998) and better access to subsurface water storage (Zhang et al., 2018). Both changes might have led to increased evapotranspiration and a reduction in streamflow.

205 3.3.2 Data Sources

We required an approach to estimate seasonal and annual evapotranspiration for the periods before and after 2000. Multiple approaches have been developed to estimate evapotranspiration (ET) using remote sensing products, but few provide robust estimates that would allow consistent comparisons of the the pre- and post-2000 periods. For instance, MODIS provides an 8-day ET product (Mu et al., 2013), but this dataset is only available since the launch of the Terra satellite in late 1999. The 210 surface energy balance approach (SEBAL, Bastiaanssen et al., 1998) can be used to estimate ET from Landsat imagery prior to 2000, but relatively few Landsat images were available during this time period and the instantaneous nature of SEBAL may therefore present biased estimates of seasonal ET.



We therefore applied a regression framework based on the concept of reference evapotranspiration (Allen et al., 1998), where evapotranspiration is defined as $ET = ET_0 \times k$. In this equation, actual evapotranspiration (ET) is characterized by a
215 reference evapotranspiration (ET_0) and mediated by a crop coefficient (k), which respectively capture the effect of climate and land use (i.e., vegetation). For calculating reference ET, we used the Hargreaves equation (Hargreaves and Samani, 1985), which provides estimates of ET_0 at monthly timescales or larger. The Hargreaves equation captures the effect of climate drivers and accounts for extraterrestrial radiation (R_a), air temperature (T_A), and the diurnal temperature range (T_R):

$$ET_0 = 0.0023R_a(T_A + 17.8)\sqrt{T_R}. \quad (1)$$

Extraterrestrial radiation R_a varies seasonally with changing solar declination angles which are associated with latitude and
220 topography. The diurnal temperature range T_R depends on a variety of climate conditions including humidity, soil moisture, precipitation, and cloud cover (Dai et al., 1999; Geerts, 2003). We group these parameters into a single seasonal parameter, $a_s \propto R_a T_R^{0.5}$, which represents mean climate conditions within each season and captures the seasonal variability in the Upper Jhelum watershed. We assume that the greenness of the vegetation canopy exerts the primary control on the stomatal conductance, such that we can define the crop coefficient as $k \approx NDVI^c$, where c is a calibrated parameter. This assumption is
225 supported by empirical evidence (Duchemin et al., 2006; Groeneveld et al., 2007). We can therefore re-write the equation for evapotranspiration in the form of a nonlinear regression:

$$ET_{i,s,y} = a_s \times (T_{A,i,s} + 17.8) \times NDVI_{i,s,y}^c + \varepsilon_{i,s,y} \quad (2)$$

where $ET_{i,s,t}$ is average MODIS ET for an individual pixel i in season s and year y , $T_{A,i,s}$ is the interpolated post-2000 seasonal average air temperature (See Sect S3), and $NDVI_{i,s,y}$ is the average Landsat NDVI for the same year-season-pixel combination. The regression coefficients a_s represent the estimated average effect of extra-terrestrial radiation R_a and diurnal
230 temperature range T_R , and c mediates the effect of NDVI on the the crop coefficient. These coefficients are assumed to be stationary across pixels (homogeneous) and years (stationary). We used a cross-validation analysis to evaluate how robust our ET estimates were to uncalibrated data. A calibration sample was formed by independently drawing 80% of pixels from each image, which we used to to estimate the regression coefficients a_s and c . The estimated coefficients were then used to predict ET on the remaining 20% of the pixels using Equation 2. Predictions matched ET observation on the validation with a high
235 degree of accuracy ($R^2 = 0.87$).

The cross-validation analysis results allowed us to build confidence in our assumptions that c and a_c were stationary and homogeneous. We relied on these assumptions to predict pre-2000 ET using Equation 2 and regression coefficients a_s and c estimated using post-2000 observations.

Finally, Strahler et al. (1999) provide annual classification of 17 land use categories using MODIS imagery. We combined
240 these categories into six super classes to represent major land use categories within the watershed: grassland and shrubs, forest, cropland, mosaic vegetation, open water (lakes), urban, and barren land. Within the Upper Jhelum, the mosaic vegetation class indicates the presence of orchard plantations (see Fig. S4). Land use change involving the cropland and mosaic classes are therefore likely to have an outsize effect on ET in the watershed, representing the primary component of locally-driven



anthropogenic changes. We used the MODIS land cover classification from 2001 (the earliest available year) to approximate
245 land use prior to the observed hydrological change, and the land classification from 2010 to represent land use after the change.

3.4 Catchment storage

3.4.1 Hypotheses

The Upper Jhelum contains a variety of storage reservoirs including surface water bodies, groundwater, snow, and glaciers
(Figure 1 d-g). From the water balance, a decrease in storage (e.g., glacial melt) must be matched by a corresponding increase in
250 the outgoing fluxes, evapotranspiration or streamflow. As such, a long-term decrease in catchment storage could have produced
a corresponding increase in streamflow followed by a similar decrease as catchment storage stabilizes. We hypothesize that
there could have been a long-term reduction in permanent water storage leading to a subsequent decline in streamflow. For
instance:

- Hypothesis 6: A long-term decline in glaciers produced an increase and subsequent decrease in streamflow
- 255 – Hypothesis 7: A long-term decline in permafrost produced an increase and subsequent decrease in streamflow

These hypotheses are grounded in studies of other catchments showing that a warming climate could temporarily increase
streamflow through glacial loss (Singh and Kumar, 1997; Schaner et al., 2012) or permafrost melting (Kurylyk et al., 2016;
Qiang et al., 2019). Such changes have been predicted to occur in high-elevation montane regions and could have contributed
to the increase in streamflow in the 1980s and 1990s and subsequent decline after 2000 (Figure 1c).

260 In addition to these long term effects, catchment storage at the *seasonal* time scale scale creates a time lag between precipi-
tation and streamflow. Understanding how snow cover, groundwater, and surface water storage have changed over time would
provide additional insight into the processes governing hydrological change in the catchment. Specifically, we hypothesize
that:

- Hypothesis 8: Reduced snow cover and earlier snow melt generated an earlier peak in annual hydrograph.
- 265 – Hypothesis 9: Reduced groundwater recharge led to a reduction in the baseflow contribution to streamflow throughout
the watershed.

All things being equal, earlier snow melt would tend to increase the amount of streamflow early in the year and decrease
streamflow later in the year. Earlier snow melt would also allow greater vegetation activity and evapotranspiration earlier in
the spring, thereby reducing groundwater recharge. In aggregate, the processes involved in these two hypotheses might have
270 increased the proportion of annual precipitation exiting the catchment as evapotranspiration instead of streamflow.

3.4.2 Data sources: Glaciers and permafrost

High altitude hillslopes and mountain peaks in the Upper Jhelum exhibit sufficiently cold annual temperatures to support both
glaciers and permafrost. In particular, Kolahoi glacier sits along the northeastern edge of the watershed and has been melting



over recent decades. The glacier was approximately 14.5 km² in 1962 and 11.3 km² in 2014 (Shukla et al., 2017). We rely on
275 estimates of glacial mass lost from published studies to determine whether these losses are sufficient to explain the observed
variations in streamflow (Sect 4).

We also consider the potential for loss of permafrost to have produced an increase and subsequent decrease in streamflow.
For example, Qiang et al. (2019) found that melting permafrost generated a temporary increase in streamflow in the upper
Yellow river of 5%. To evaluate the possibility for this process in the Upper Jhelum, data were downloaded from the Global
280 Permafrost Zonation Index (GPZI) map (Gruber, 2012). Given the uncertainty in permafrost occurrence, the GPZI is presented
on a scale that indicates the likelihood of permafrost, with a minimum indicating that “permafrost exists only in most favorable
conditions” and maximum indicating that “permafrost exists in nearly all conditions.” We binned this scale into five groups
of permafrost likelihood including low, medium-low, medium, medium-high, and high. The upper Jhelum contains no pixels
with medium-high or high likelihood of permafrost and in most of the areas where permafrost is possible, the likelihood is low
285 (see Fig. S8). To evaluate the potential for permafrost to affect streamflow, we compared the areal extent of the GPZI with the
necessary loss of frozen water storage to produce the observed changes in streamflow.

3.4.3 Data sources: Snow

Winter precipitation occurs largely as snowfall and remains in some parts of the catchment until the late summer. Because
different regions of the watershed may be affected by missing pixels (e.g., clouds) on any given acquisition date, we separated
290 the watershed into 15 distinct zones of roughly equal areas defined by three elevation bands (<1650 m, 1650–2200 m, and
>2200 m) in the five local subwatersheds corresponding to the available stream gauges. Snow contains a distinct spectral
signature with high reflectance in visible and near-infrared bands and low reflectance in shortwave infrared bands, and can
therefore be detected by from normalized different snow index (NDSI), which is defined as (Green - SWIR)/(Green + SWIR)
(Dietz et al., 2012). We generated timeseries of snow cover in each of the 15 zones using Landsat 5 imagery by applying a
295 threshold of 0.5 to NDSI to distinguish snow and water cover from dry land. We further distinguish snow (bright) from open
water (dark) using a threshold of 0.2 on the NIR band reflectance (Kulkarni et al., 2002). For each zone, we selected only
the dates where missing pixels constituted less than 25% of the zone, leaving an average of 79 and 65 observations in each
zone before and after 2000, respectively. We generated an adjusted snow estimate for each zone and date by dividing raw
snow cover estimates by the fraction of missing pixels. We then estimated average daily snow cover by fitting locally weighted
300 non-parametric time regressions (LOESS) (Cleveland et al., 1992) to snow cover observations, for each zone, before and after
2000. The final smoothed estimate of snow cover was taken as the sum of snow cover across all zones, with 95% confidence
intervals calculated from the sum of standard errors across the zones.

3.4.4 Data sources: Groundwater

We were unable to obtain *in situ* groundwater observations and remotely sensed observations from GRACE satellite were
305 inadequate due the large spatial averaging kernel ($\approx 40,000$ km², compared to a catchment area of approximately 13,000 km²)
and lack of observations prior to 2002. We therefore relied on proxies to assess changes in groundwater behavior.



First, we considered changes in baseflow discharge an indication of changes in groundwater. Commonly applied (non-)linear reservoir models assume that baseflow discharge follows a monotonic relationship with groundwater storage. Therefore a change in baseflow over time (see Sect. 2.2) would indicate a change in groundwater storage.

310 Second, we looked for hysteresis in the relationship between surface water storage and streamflow as indicative of a ground-water surface water connectivity. We assumed that high groundwater levels in the riparian sedimentary aquifer would allow it to be hydrologically connected to the lakes and wetlands in the valley bottom. A weak or non-existent hysteresis might be indicative of a weak influence of groundwater on streamflow, whereas a strong hysteresis would indicate both a greater influence of groundwater and the occurrence of meaningful fluctuations in the water table, including the possibility that the water table
315 might periodically disconnected from the surface water system. We evaluated possible hysteresis before and after 2000 using the results of the surface water classification and the trimonthly timeseries of streamflow directly downstream of the surface reservoirs.

3.4.5 Data sources: Surface water

A number of lakes and wetlands exist throughout the valley including Wular lake, which intersects the main stem of the Upper
320 Jhelum between gauges (iii) and (iv), and seasonally inundated valley wetlands which capture flow from the subwatershed that drains into gauge (iv) (see Fig. 1). The actual volumetric surface water storage of the catchment is difficult to estimate. Instead, we focus on changes in surface water area using remote sensing imagery. We classify surface water extent in Wular lake and in the wetlands in all available Landsat imagery over the period 1984–2013.

Open water is highly absorptive in short-wave infrared bands and more reflective in bands with shorter wavelengths. We
325 use the modified normalized-difference water index (MNDWI Xu, 2006) as an indication of the likelihood of open surface water, with a threshold distinguishing between land and water pixels. Because water exhibits spatial coherence dictated by topography, we gap-filled missing pixels in Landsat 7 bands due to the scan-line corrector error by propagating edge pixels towards the center of the gap (as in Penny et al., 2018). We used a fixed MNDWI threshold across all images to classify surface water. Clouds were identified using the rudimentary Simple Cloud Score algorithm in Google Earth Engine
330 (`ee.Algorithms.Landsat.simpleCloudScore()`) on top-of-atmosphere images. We applied this classification approach to 66 images (Landsat 5) before 2000 and 237 images (Landsat 5 & 7) after 2000 for Wular lake and valley inundation.

4 Results

Our estimates of rainfall, streamflow, evapotranspiration and storage change allowed the water balance to be closed for the 1984-1999 and 2000-2013 periods with an error of $\pm 15\%$ (Fig. 3). This suggests that the total watershed fluxes are estimated
335 with reasonable confidence, particularly given uncertainty in rainfall interpolation and remote sensing models of evapotranspiration.

However, the analysis did not allow us to close the differential water balance (i.e., changes in the water balance) between the two periods. We observed an average decrease in precipitation of 117 mm per year and an increase in ET of 32 mm per year,

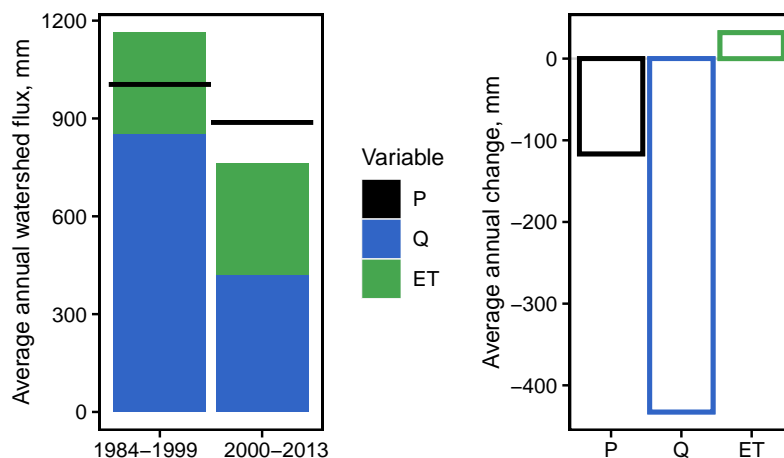


Figure 3. Water balance for the Upper Jhelum. (left) Average annual fluxes (P, Q, and ET) for the periods 1984–1999 and 2000–2013. (right) Average annual *change* in water balance fluxes between the two periods.

which together do not close the observed decrease in streamflow of 433 mm per year. We do not find evidence of a change
340 in long term storage processes (e.g., decrease in glacial melt) that would close the balance. The issue, therefore, appears that
biases on individual watershed fluxes (e.g., an equivalent underestimation of P and ET) might compensate each other and close
the water balance at individual periods, while underestimating the components of *changes* in Q. This issue illustrates the limits
of a top-down approach, where attribution of hydrological change relies on the predictive ability of an aggregate hydrological
model, including one as simple as the catchment-scale water balance. Closing the differential water balance would have allowed
345 to attribute the observed changes in streamflow to corresponding changes in other fluxes. In contrast, the bottom up approach
to attribution does not rely on our ability to close the differential water balance. Instead, the hypotheses developed above
(Section 3) are investigated individually, as described below. While data limitations might prevent a subset of the hypotheses
from being conclusively tested, the approach nevertheless reveals a process-based understanding of hydrological change in the
Upper Jhelum watershed.

350 4.1 Precipitation: hypotheses 1-3

Precipitation exhibited notable changes in total volume, as annual precipitation fell by 117 mm, corroborating *Hypothesis 1*.
Precipitation also exhibited changes across seasons (Fig. 4), consistent with *Hypothesis 2*. These changes were driven almost
entirely by a loss of spring precipitation of 117 mm. The other seasons saw modest and statistically insignificant changes in
precipitation (+20 mm in winter, -14 mm in summer, -5 mm in autumn).

355 Additionally, the number of storms greater than 1 mm increased in all seasons except spring, thus supporting *Hypothesis 3*
(Fig. 4c). Combined with the fact that precipitation either decreased or remained constant, this entails a *decrease* in average

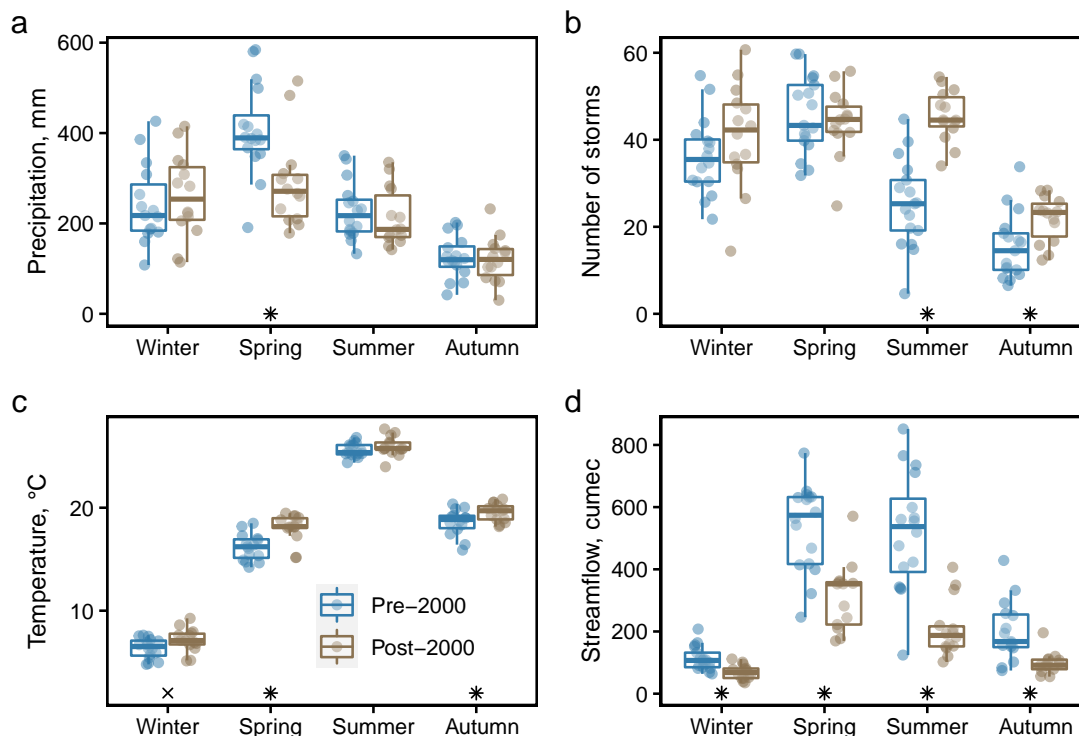


Figure 4. Seasonal climate and hydrology in the Pre-2000 (1984–1999) and Post-2000 (2000–2013) periods including (a) mean seasonal gauge precipitation, and (b) mean number of storms greater than 1 mm in PERSIANN grid cells, (c) mean gauge temperature, and (d) mean streamflow at the watershed outlet (gauge v, Baramulla station). Statistically significant differences from t-tests are noted for $p < 0.05$ (*) and $p < 0.1$ (x). Notably, spring exhibited dramatic changes in temperature (+1.9°C) and precipitation (-117 mm). The number of storms increased in summer and autumn, yet remained relatively constant in spring. Reductions in streamflow were statistically significant in all seasons.

storm size across all seasons. The implications of these findings in relation to the water balance are revisited in the Discussion (Sect. 5).

4.2 Evapotranspiration: hypotheses 3-4

360 Annual average watershed evapotranspiration increased by 32 mm, from 311 mm before 2000 to 343 mm after 2000. The two hypotheses pertaining to ET seek to attribute this increase to either changing climate or changing land use. Both drivers have contributed to ET increase in the catchment, as indicated by increases in both air temperature and the NDVI. Based on simple averages of gauge data, temperature increased significantly in winter (+0.8°C), spring (+1.9°C), and autumn (+1.0°C, Fig. 4).

The most dramatic increases in ET occurred within agricultural land cover classes (cropland and mosaic vegetation, i.e. 365 orchards), which constituted 27% of the catchment area in 2001. In these classes, NDVI increased substantially in the spring and

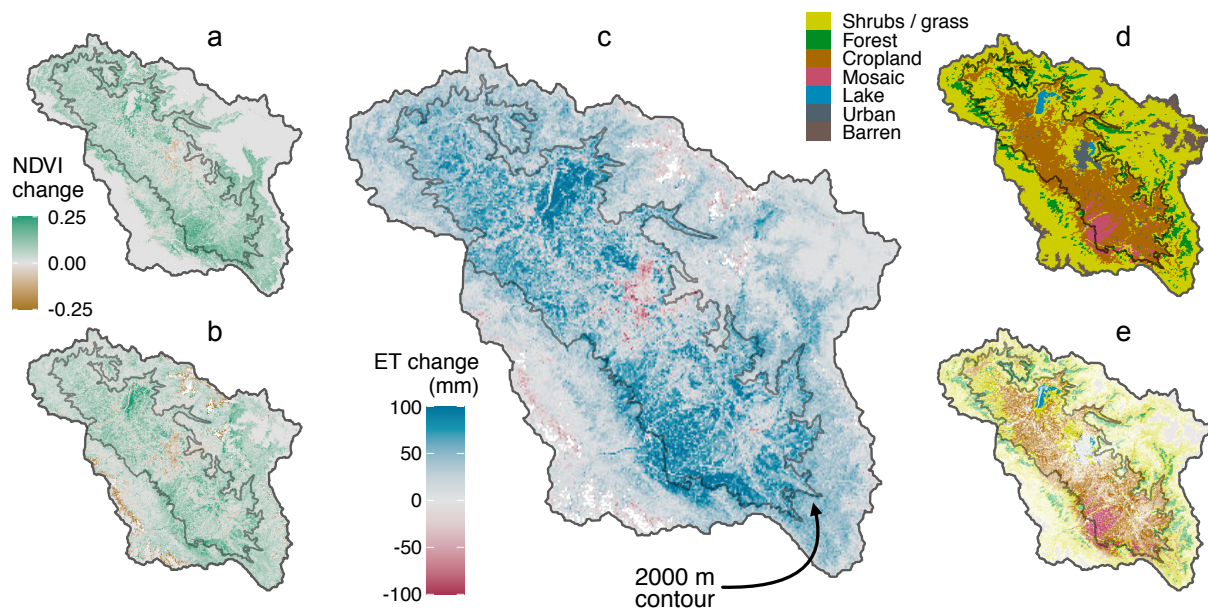


Figure 5. Spatial changes in evapotranspiration after 2000. (a) Spring and (b) summer changes in NDVI. (c) Annual change in evapotranspiration (ET). (d) MODIS land cover map from 2010. (e) The same MODIS 2010 land cover map, with pixel transparency determined by the magnitude of positive change in annual ET from (c). The 2000 m contour separates the low-elevation valley from moderate elevation hillslopes in both mountain ranges. Changes in ET are clustered in the valley, especially in cropland and mosaic vegetation (i.e., orchards), with increasing ET in natural vegetation just above 2000 m. See text for details.

summer seasons (Fig. 5). Between 2001 and 2011, the catchment exhibited notable expansion of the mosaic land cover class, including approximately 230 km² converted from traditional crops to mosaic. The largest local increases in ET are associated with this expansion, including land cover transitions to mosaic vegetation (see Fig. 6a), with ET increasing by 70 mm (mosaic to mosaic), 78 mm (cropland to mosaic), and 82 mm (shrubs and grassland to mosaic). In addition, noticeable increases in ET

370 also occurred in the large portion of the watershed area (53%) that was consistently classified as shrubs and grassland in both 2001 and 2011. NDVI increased along the hills on the southwest and northeast portions of the watershed, resulting in higher ET in grassland / shrubs and forest land cover. NDVI remained constant in the Wular lake in spring but increased considerably in summer, likely due to increasing fertilizer application supporting algae and other aquatic vegetation in the lake (Wetlands International South Asia, 2007). In contrast, regions where NDVI appears to have decreased are dominated by urbanization in

375 the center of the valley (visible in Fig 5ab) and mountain peaks with near-constant cloud cover in the summer, which occur along the southeastern and northwestern watershed boundaries. In these pixels, few (≤ 5) summer NDVI observations are available before 2000 due to cloud cover, suggesting a substantial level of uncertainty in the reported negative NDVI trend (see Fig. S6).

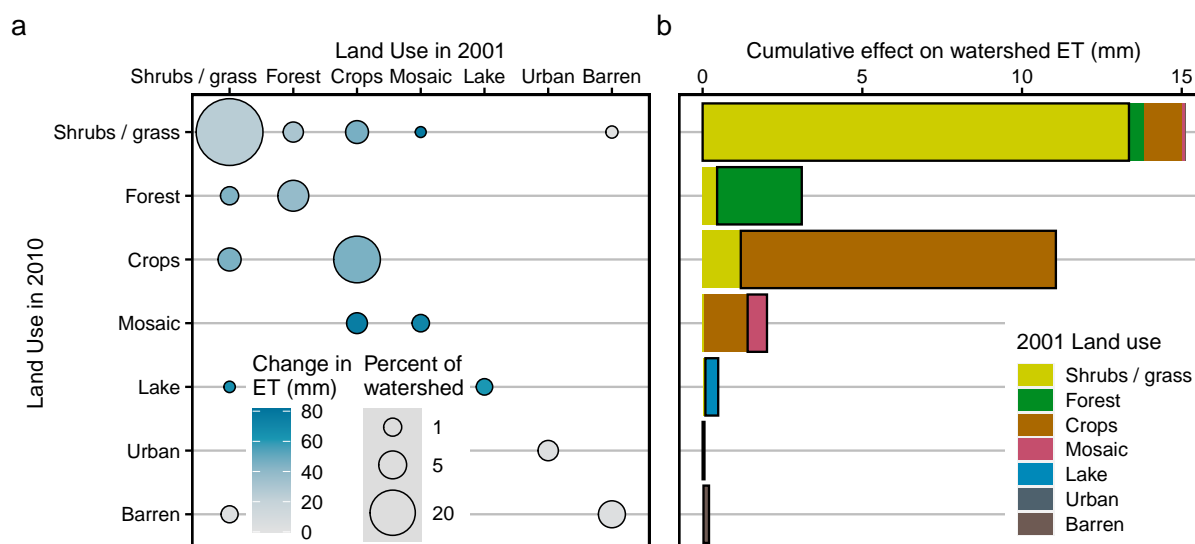


Figure 6. Changes in land use and evapotranspiration. (a) MODIS Land use change from 2001 to 2010, including the average increase in evapotranspiration within each combination of categories. (b) Watershed average effect of each land use category on evapotranspiration. Most of the increase in watershed ET (27 mm) occurred in regions where land cover remained consistent from 2001 to 2010 (outlined in black), compared with regions where land cover changed (5 mm).

Overall, of the 32 mm annual increase in ET that we detected, approximately 17% can be attributed directly to increasing air temperature, and the remaining 83% to an increase in NDVI. The largest net contributors to watershed-averaged increases in ET were shrubs and grassland (15 mm), cropland (11 mm) and forest (3 mm). Although associated with strong local increases in evapotranspiration, mosaic vegetation covered only 2.7% of the watershed in 2011 and only contributed a 2 mm increase to watershed-average ET. The black boxes in Fig 6b encompass the change in ET for regions of the watershed that maintained consistent land cover in 2001 and 2010, accounting for a total increase in ET of 27 mm compared with 5 mm in regions where land cover changed. We can therefore say that climate change had a clear effect on watershed evapotranspiration, both through increasing temperature and increasing NDVI within naturally vegetated land classes, consistent with *Hypothesis 4*. Regarding *Hypothesis 5*, land use change has led to large local increases in ET. However, the overall effect on the catchment water balance is small compared to climate-related increases of ET in the much higher number of remaining pixels where land use did not change between 2000 and 2011.

390 4.3 Catchment storage: hypotheses 6-9

Observational records indicate decreasing water storage over time in the Upper Jhelum. Kolahoi glacier has lost considerable volume over time, estimated as 0.3 km³ in the period 1962-2013 (Rashid et al., 2017). This corresponds to an average loss of 23.3 m thickness across the glacier over the entire five decades, or 0.456 m year⁻¹ loss in glacial thickness. Because the glacial



395 extent is approximately 0.1% of the catchment area (Shukla et al., 2017), such losses would amount to $0.456 \text{ mm year}^{-1}$ of
annual streamflow at the outlet of the Jhelum. These losses are several orders of magnitude smaller than the observed changes
in streamflow, allowing us to reject *Hypothesis 6*.

Overall, roughly 0.19% of the watershed has at least a medium likelihood of permafrost (Fig. S8). In a larger portion (6.4%)
permafrost has a low likelihood and therefore requires extremely favorable conditions and is therefore likely to be shallow
(Gruber, 2012). In that context, the 50 mm per year increase in Upper Jhelum streamflow necessary to close the differential
400 water balance would require a loss of 780 m per year of permafrost in all regions where permafrost is likely to be shallow. Such
a permafrost loss is orders of magnitude greater than observed changes in permafrost in other basins. For example in upper
reach of the Yellow River Basin where Qiang et al. (2019) estimated less than 1 cm loss of ground ice per year. We conclude
that permafrost cannot be considered an important driver of changes in streamflow and we can reject *Hypothesis 7*.

Snow cover follows a seasonal signal, with a maximum in late winter followed by receding snow pack in spring. After
405 2000, the maximum snow cover cover extent was reduced and was followed by more rapid snow melt (Fig. 7a). The extent of
the influence of snow on the hydrograph appears to be reflected by an earlier peak in the hydrograph. This finding supports
Hypothesis 8, although observational data is missing to quantify the implicated changes in storage volumes. Earlier snow-melt
and its hypothesized effect on the water balance is nonetheless consistent with the observed increased in ET during the spring
(see Sect. 5 for further discussion).

410 Remote sensing observations of open water extent suggests that surface water storage declined dramatically during the study
period, both in Wular lake and the neighboring wetlands (Fig. 7b). Both of these surface reservoirs connect to the main stem of
the Upper Jhelum between gauges iii. and iv. (see Fig. 1), and likely play an important role in streamflow generation along this
reach. To investigate this effect, we computed locally generated baseflow as the difference in baseflow between gauges iii. and
iv. Baseflow along this reach peaks earlier and at a much lower amplitude after 2000 (Fig. 7c). It also transitions much earlier
415 (mid-summer) to losing conditions (i.e. negative local streamflow values), compared to pre-2000 where baseflow transitioned to
losing conditions only at the end of autumn and beginning of winter. Additionally, the relationships between locally generated
baseflow and open water extent (of the lake and the wetlands) exhibit a seasonal hysteresis (see Fig. S7), which we interpret as
indication that groundwater plays an important role mediating streamflow generation in the valley bottom. Although the shape
of the hysteresis remains similar, the amplitude of the hysteresis behavior is reduced considerably after 2000.

420 The implication of changing groundwater storage can be better understood by comparing temporal trends in streamflow
below Wular lake (iv., Sopore station) and the most upstream gauge of the watershed (i., Sangam station). The streamflow
timeseries at both locations exhibit statistically significant decreasing trends over the period 1960–2013 (Fig. 8a). Baseflow
separation, however, reveals important differences between both streamflow timeseries. Baseflow decreases over time only in
the downstream gauge (Fig. 8b) whereas quickflow decreases only in the upstream gauge (Fig. 8c). Temporal changes in the
425 baseflow index ($B = Q_B/Q_{Total}$) of each of these gauges therefore occurs in opposite directions, with decreasing B near the
outlet and increasing B in the hinterlands (Fig. 8d). This lends credence to *Hypothesis 9*, and we further discuss potential
causes and implications of these opposing trends in the baseflow index with respect to saturated and unsaturated groundwater
storage in the Discussion (Sect. 5).

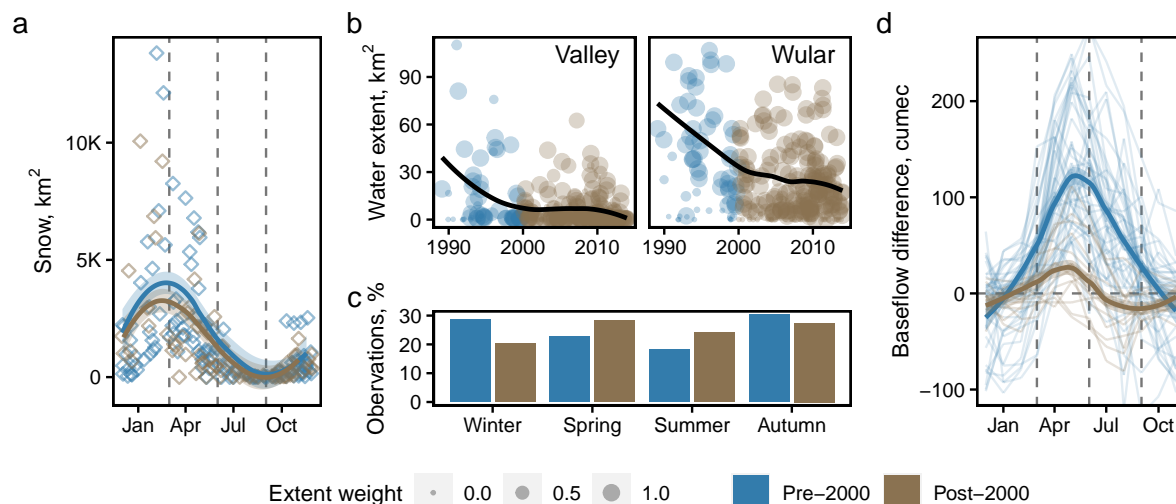


Figure 7. Declining water storage and baseflow. (a) Landsat observations of snow cover with loess smoothing, highlighting earlier spring snowmelt after 2000. (b) Long-term trends in valley inundation and Wular lake indicating decreasing surface water storage over time. The loess smoothing of water extent is weighted by cloud cover given by $\exp(-A_{cloud}/A_{total})$. (c) The percent of satellite images used to assess water extent was seasonally consistent before and after 2000. (d) Baseflow at gauge iv. (Sopore) minus baseflow at gauge iii. (Asham), encompassing the river reach that includes Wular lake. After 2000, baseflow peaks and depletes earlier in the year, as does a transition from gaining to losing conditions.

5 Discussion

430 We now synthesize the results presented above to develop a narrative of hydrological change by reconciling the various fluxes that have either increased or decreased over time (Fig. 9, red and blue arrows). Taken together, the observed changes in hydrological fluxes indicate additional unobserved changes in fluxes connecting surface and groundwater that might play an important role in explaining hydrological change in the catchment. As discussed in the following paragraphs, evidence suggests that these fluxes have decreased over time (Fig. 9, pink arrows).

- 435 – The largest seasonal precipitation occurs in spring, when the prevailing climate is driven by westerlies, yet spring precipitation declined considerably during the study period. At the same time, vegetation activity increased across most of the watershed within both anthropogenic (cropland, orchards) and natural (forest, shrubs and grassland) land use classes (Fig 5a), producing an increase in evapotranspiration. The corresponding reduction in spring streamflow was partially compensated by higher temperatures and earlier snow melt. Near the end of the study period, the snow pack was nearly
- 440 always exhausted by the end of spring (Fig 7a).

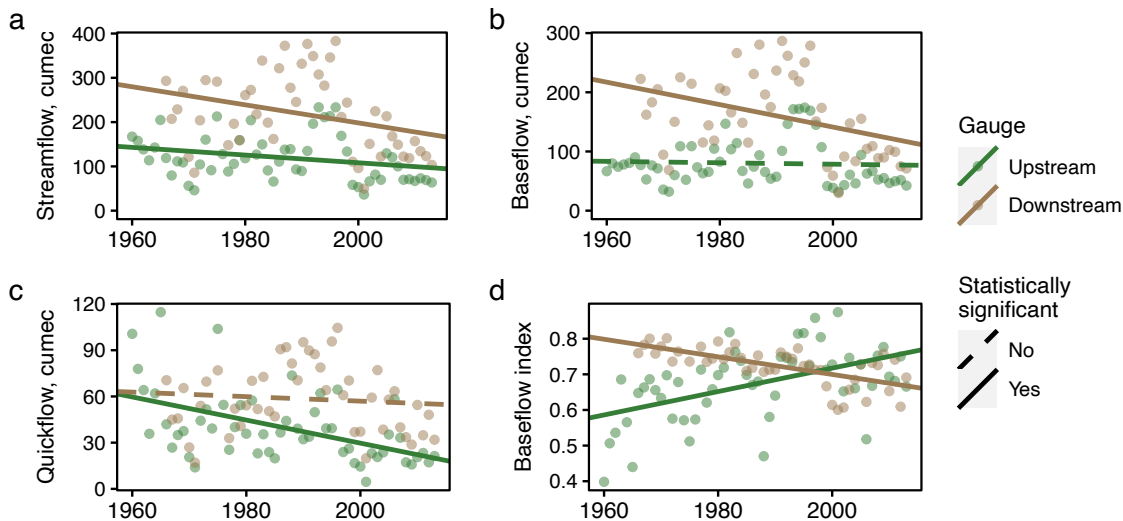


Figure 8. Long-term trends at Sangam station (upstream, gauge i.) and Sopore station (downstream, gauge iv.) of (a) streamflow, (b) baseflow, (c) quickflow, and (d) the baseflow index, which is the fraction of streamflow comprised of baseflow.

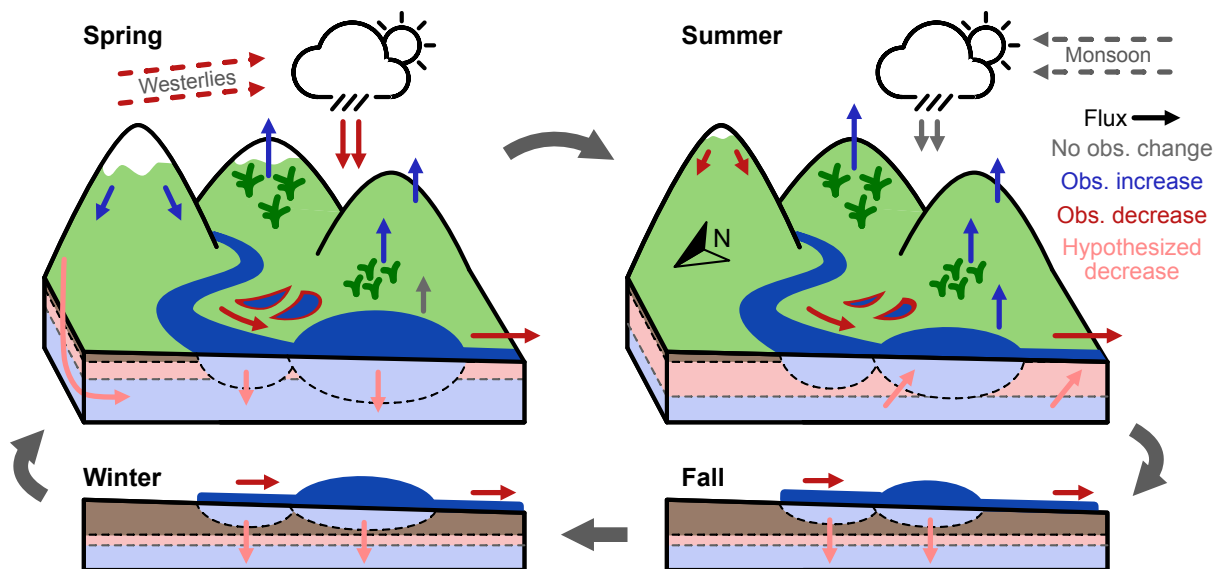


Figure 9. Conceptual diagram of seasonal water fluxes and direction of change. Black, red, and blue arrows indicate observed fluxes combined with the observed sign of change. Pink arrows indicate groundwater fluxes that have been inferred and hypothesized to decrease over the study period. See text for details.



- Springtime seepage generates high groundwater recharge throughout the valley, both from the highlands and from within the valley (Jeelani, 2008). High groundwater levels at the end of the spring season are reflected by the peak in baseflow along the reach of the stream that includes Wular lake (Fig. 7d). Prior to 2000, this peak occurred near the transition between spring and summer. After 2000, this peak occurred earlier in spring and at a much lower level of baseflow. This suggests considerably lower groundwater storage over time, reflected in the reduced groundwater recharge fluxes (Fig 9, Spring).
- In summer, the prevailing climate is driven by the Indian monsoon and precipitation is generally less than westerly precipitation in the spring (Fig 4a). Consequently, hydrology within the watershed is controlled largely by water storage (snow, lakes and groundwater) left over from spring. Prior to 2000, the seasonal recession of the baseflow hydrograph starts high at the end of spring and continues to produce discharge throughout the summer season (Fig 7d). The river then transitions to losing conditions in autumn and earlier winter before baseflow increases with winter precipitation and snow melt (Fig 7d). After 2000, snow pack at the beginning of summer is nearly exhausted, and surface water (Fig. S5) and groundwater (Fig. 7d) storage are also reduced. The receding limb of the hydrograph starts low at the beginning of summer and quickly depletes, transitioning to losing conditions within the summer season. Indeed, the recovery of local baseflow in autumn (i.e., baseflow becoming less negative, see Fig. 7d, brown) is driven by declining baseflow downstream rather than increasing baseflow upstream. Additionally, summer evapotranspiration after 2000 increased throughout much of the watershed including in natural and anthropogenic land use classes.
- The hydrological cycle in the watershed is mostly dormant in autumn and winter. In autumn, little precipitation falls and the hydrograph recedes into winter. Notably, lake storage depletes and the lake transitions to losing conditions in several years, particularly before 2000 (Fig. 7d). Winter precipitation arrives mostly as snowfall, replenishing snow storage. Winter rain and snow melt serve as the early primers for the seasonal cycle to renew in spring.

To summarize, climate appears to be the primary cause of hydrological change within the Upper Jhelum. The most influential driver is the decline of spring westerly precipitation. Other studies have associated this decrease with warming temperatures (Zaz et al., 2019). This effect is compounded by an array of other drivers that affect watershed processes. Notably, the loss of baseflow downstream of Wular lake suggests a decrease in groundwater storage in the valley. This decline in groundwater is facilitated both by reduced rainfall during the spring and increasing watershed evapotranspiration. The latter might be exacerbated by an *increase* in the number of storms for precipitation falling outside of the spring season. This observation from the PERSIANN CDR dataset allows us to hypothesize that the shift towards a larger number of smaller storms results in reduced overland and macropore flow, along with more stable and persistent soil moisture and ultimately more water “lost” to vegetation uptake. In this case, seepage would be increasingly likely to occur via slow drainage processes, rather than macropore flow activated in large storms. Such changes have been observed in other karst catchments (Zhao et al., 2019) and are supported by the evidence that quickflow declined and the baseflow index increased in the most upstream gauge in the Upper Jhelum (Fig. 8). The increase in evapotranspiration appears to have occurred throughout the catchment. Our evapotranspiration model indicates that increasing air temperature had a small direct effect on ET (a 2% increase) and that most of the overall



475 increase in ET (83%) occurred due to changes in NDVI, which increased in all natural and anthropogenic vegetation classes. The climate signal therefore manifested itself by providing favorable conditions for plant biomass growth, as represented by increasing greenness. Such a change would be expected with warming temperatures and reduced snow cover early in the year, in addition to greater energy availability (temperature) and water availability (soil moisture) that arose due to climate warming and increased storm frequency, respectively. Evapotranspiration exhibited the greatest increases in regions that transitioned to
480 orchard cultivation, but these areas represent a small fraction of the overall watershed and increase in ET. Evapotranspiration also increased considerably in cropland areas, likely due to the aforementioned climatic changes in addition to agricultural intensification. Indeed, increasing fertilizer use in the catchment has been noted in other studies (Wetlands International South Asia, 2007) and might have contributed to the increased ET in agricultural land use classes. It is also an important driver contributing to the growth of aquatic vegetation and increasing ET in Wular lake in the summer (see Figs 5,6).

485 6 Conclusions

In this study, we develop a bottom-up approach to hydrological attribution to understand the drivers of dramatic changes in the annual streamflow of the Upper Jhelum river. We found that much of the observed decrease in streamflow is associated with decreases in westerly precipitation in spring, in addition to greater evapotranspiration. While land-use change to orchard plantations and agricultural intensification are likely contributing factors, we attribute most of the increase in evapotranspiration
490 to non-local anthropogenic causes, most notably increased vegetation activity in spring due to increased temperature and earlier snow melt.

The approach focuses on the development of a process understanding of hydrological change in the catchment by separately evaluating multiple hypotheses about specific mechanisms, rather than relying on a basin-wide aggregate model for predictive inference. As such, it is a promising tool to attribute hydrological change in situations where process uncertainty might be
495 compounded by hydrologic regime shifts. Additional uncertainty in the water balance, due to bias in hydrological observations, limits the utility of catchment-scale models, including a model as simple as the water balance. Indeed, detection biases associated the different remote sensing sources might compound and prevent the proper calibration of an aggregate model, as seen in our inability to close the differential water balance. Instead of being used as a predictive tool, the water balance (or any other conceptual model) is here used as a framework to generate hypotheses that can be investigated individually. While
500 outcomes associated with individual hypotheses might exhibit considerable uncertainty, especially in data-scarce catchments, together the multiple hypotheses provide multiple strands of evidence to support (or refute) specific mechanisms and ultimately attribute hydrological change.

Data availability. The secondary data that support the findings of this study are available on request from the corresponding monitoring and collection agencies. Remote sensing products used in this study are freely available from the respective providers (see in-text citations).



505 *Author contributions.* G.P., Z.A.D., and M.F.M designed the research, G.P. conducted the analyses, G.P. and M.F.M wrote the paper

Competing interests. The authors declare that they have no conflict of interest

Acknowledgements. G.P. and M.F.M. acknowledge support from the National Science Foundation under Grant No. ICER 1824951.



References

- Aeschbach-Hertig, W. and Gleeson, T.: Regional strategies for the accelerating global problem of groundwater depletion, *Nature Geoscience*, 5, 853–861, <https://doi.org/10.1038/ngeo1617>, 2012.
- Akhter, M.: The Political Ecology of the Water Scarcity / Security Nexus in the Indus Basin: Decentering Per Capita Water Supply, pp. 21–33, <https://doi.org/10.1007/978-3-319-32845-4>, 2017.
- Alexandratos, N.: Countries with rapid population growth and resource constraints: issues of food, agriculture, and development, *Population and development Review*, 31, 237–258, 2005.
- 515 Allen, R. G., Pereira, L. S., Raes, D., Smith, M., et al.: Crop evapotranspiration-Guidelines for computing crop water requirements-FAO Irrigation and drainage paper 56, Fao, Rome, 300, D05 109, 1998.
- Ashouri, H., Hsu, K.-L., Sorooshian, S., Braithwaite, D. K., Knapp, K. R., Cecil, L. D., Nelson, B. R., and Prat, O. P.: PERSIANN-CDR: Daily precipitation climate data record from multisatellite observations for hydrological and climate studies, *Bulletin of the American Meteorological Society*, 96, 69–83, 2015.
- 520 Badar, B., Romshoo, S. A., and Khan, M. A.: Modelling catchment hydrological responses in a Himalayan Lake as a function of changing land use and land cover, *Journal of Earth System Science*, 122, 433–449, <https://doi.org/10.1007/s12040-013-0285-z>, 2013.
- Bastiaanssen, W. G., Menenti, M., Feddes, R., and Holtlag, A.: A remote sensing surface energy balance algorithm for land (SEBAL). 1. Formulation, *Journal of hydrology*, 212, 198–212, 1998.
- Beven, K.: A manifesto for the equifinality thesis, *Journal of Hydrology*, 320, 18–36, <https://doi.org/10.1016/j.jhydrol.2005.07.007>, 2006.
- 525 Ceola, S., Laio, F., and Montanari, A.: Global-scale human pressure evolution imprints on sustainability of river systems, *Hydrology and Earth System Sciences*, 23, 3933–3944, <https://doi.org/10.5194/hess-23-3933-2019>, 2019.
- Chamberlin, T. C.: The method of multiple working hypotheses, *Science*, 148, 754–759, <https://doi.org/10.1126/science.148.3671.754>, 1965.
- Chan, S. K., Bindlish, R., O'Neill, P. E., Njoku, E., Jackson, T., Colliander, A., Chen, F., Burgin, M., Dunbar, S., Piepmeier, J., et al.: Assessment of the SMAP passive soil moisture product, *IEEE Transactions on Geoscience and Remote Sensing*, 54, 4994–5007, 2016.
- 530 Cleveland, W., Grosse, E., and Shyu, W.: Local regression models. Chapter 8 in *Statistical models in S* (JM Chambers and TJ Hastie eds.), 608 p, Wadsworth & Brooks/Cole, Pacific Grove, CA, 1992.
- Dai, A., Trenberth, K. E., and Karl, T. R.: Effects of clouds, soil moisture, precipitation, and water vapor on diurnal temperature range, *Journal of Climate*, 12, 2451–2473, 1999.
- Dar, R. A., Romshoo, S. A., Chandra, R., and Ahmad, I.: Tectono-geomorphic study of the Karewa Basin of Kashmir Valley, *Journal of Asian Earth Sciences*, <https://doi.org/10.1016/j.jseaes.2014.06.018>, 2014.
- 535 DES: Annual season crop report for 1970-2015, Directorate of Economics and Statistics, 2015.
- Dey, P. and Mishra, A.: Separating the impacts of climate change and human activities on streamflow: A review of methodologies and critical assumptions, *Journal of Hydrology*, 548, 278–290, <https://doi.org/10.1016/j.jhydrol.2017.03.014>, 2017.
- Dietz, A. J., Kuenzer, C., Gessner, U., and Dech, S.: Remote sensing of snow—a review of available methods, *International Journal of Remote Sensing*, 33, 4094–4134, 2012.
- 540 Duchemin, B., Hadria, R., Erraki, S., Boulet, G., Maisongrande, P., Chehbouni, A., Escadafal, R., Ezzahar, J., Hoedjes, J., Kharrou, M., et al.: Monitoring wheat phenology and irrigation in Central Morocco: On the use of relationships between evapotranspiration, crops coefficients, leaf area index and remotely-sensed vegetation indices, *Agricultural Water Management*, 79, 1–27, 2006.



- Ehret, U., Gupta, H. V., Sivapalan, M., Weijs, S. V., Schymanski, S. J., Blöschl, G., Gelfan, A. N., Harman, C., Kleidon, A., Bogaard, T. A.,
545 Wang, D., Wagener, T., Scherer, U., Zehe, E., Bierkens, M. F. P., Di Baldassarre, G., Parajka, J., Van Beek, L. P. H., Van Griensven, A.,
Westhoff, M. C., and Winsemius, H. C.: Advancing catchment hydrology to deal with predictions under change, *Hydrology and Earth
System Sciences*, 18, 649–671, <https://doi.org/10.5194/hess-18-649-2014>, 2014.
- Ferraro, P. J., Sanchirico, J. N., and Smith, M. D.: Causal inference in coupled human and natural systems, *Proceedings of the National
Academy of Sciences*, 116, 5311–5318, <https://doi.org/10.1073/pnas.1805563115>, 2019.
- 550 Flörke, M., Schneider, C., and McDonald, R. I.: Water competition between cities and agriculture driven by climate change and urban growth,
Nature Sustainability, 1, 51–58, 2018.
- Foufoula-Georgiou, E., Takbiri, Z., Czuba, J. A., and Schwenk, J.: The change of nature and the nature of change in agri-
cultural landscapes: Hydrologic regime shifts modulate ecological transitions, *Water Resources Research*, 51, 6649–6671,
<https://doi.org/10.1002/2015WR017637>, 2015.
- 555 Geerts, B.: Empirical estimation of the monthly-mean daily temperature range, *Theoretical and Applied Climatology*, 74, 145–165, 2003.
- Gober, P., White, D. D., Quay, R., Sampson, D. A., and Kirkwood, C. W.: Socio-hydrology modelling for an uncertain future, with examples
from the USA and Canada, Geological Society, London, Special Publications, 408, 183–199, 2017.
- Gorelick, N., Hancher, M., Dixon, M., Ilyushchenko, S., Thau, D., and Moore, R.: Google Earth Engine: Planetary-scale geospatial analysis
for everyone, *Remote Sensing of Environment*, <https://doi.org/10.1016/j.rse.2017.06.031>, 2017.
- 560 Groeneveld, D. P., Baugh, W. M., Sanderson, J. S., and Cooper, D. J.: Annual groundwater evapotranspiration mapped from single satellite
scenes, *Journal of Hydrology*, 344, 146–156, 2007.
- Gruber, S.: Derivation and analysis of a high-resolution estimate of global permafrost zonation, *The Cryosphere*, 6, 221–233, 2012.
- Hargreaves, G. H. and Samani, Z.: Reference Crop Evapotranspiration from Ambient Air Temperature, in: American Society of Agricultural
Engineering Meeting, Chicago, 1985, vol. 24, <https://doi.org/10.13031/2013.26773>, 1985.
- 565 Harrigan, S., Murphy, C., Hall, J., Wilby, R., and Sweeney, J.: Attribution of detected changes in streamflow using multiple working hy-
potheses, *Hydrology and Earth System Sciences*, 18, 1935–1952, 2014.
- Hussain, I. and Hanjra, M. A.: Does irrigation water matter for rural poverty alleviation? Evidence from South and South-East Asia, *Water
policy*, 5, 429–442, 2003.
- Jeelani, G.: Aquifer response to regional climate variability in a part of Kashmir Himalaya in India, *Hydrogeology Journal*, 16, 1625–1633,
570 <https://doi.org/10.1007/s10040-008-0335-9>, 2008.
- Jeelani, G., Saravana Kumar, U., and Kumar, B.: Variation of $\delta^{18}\text{O}$ and δD in precipitation and stream waters across the Kash-
mir Himalaya (India) to distinguish and estimate the seasonal sources of stream flow, *Journal of Hydrology*, 481, 157–165,
<https://doi.org/10.1016/j.jhydrol.2012.12.035>, 2013.
- Kampf, S. K. and Burges, S. J.: Quantifying the water balance in a planar hillslope plot: Effects of measurement errors on flow prediction,
575 *Journal of Hydrology*, 380, 191–202, 2010.
- Kampf, S. K., Burges, S. J., Hammond, J. C., Bhaskar, A., Covino, T. P., Eurich, A., Harrison, H., Lefsky, M., Martin, C., McGrath, D.,
Puntenney-Desmond, K., and Willi, K.: The Case for an Open Water Balance: Re-envisioning Network Design and Data Analysis for a
Complex, Uncertain World, *Water Resources Research*, 56, 1–19, <https://doi.org/10.1029/2019WR026699>, 2020.
- Kitchin, R.: *The data revolution: Big data, open data, data infrastructures and their consequences*, Sage, 2014.
- 580 Kulkarni, A., Srinivasulu, J., Manjul, S., and Mathur, P.: Field based spectral reflectance studies to develop NDSI method for snow cover
monitoring, *Journal of the Indian Society of Remote Sensing*, 30, 73–80, 2002.



- Kurylyk, B. L., Hayashi, M., Quinton, W. L., McKenzie, J. M., and Voss, C. I.: Influence of vertical and lateral heat transfer on permafrost thaw, peatland landscape transition, and groundwater flow, *Water Resources Research*, 52, 1286–1305, 2016.
- Levy, M. C., Neely, W. R., Borsa, A. A., and Burney, J. A.: Fine-scale spatiotemporal variation in subsidence across California's San Joaquin Valley explained by groundwater demand, *Environmental Research Letters*, 15, 104 083, 2020.
- Liu, J., Zhou, Z., Yan, Z., Gong, J., Jia, Y., Xu, C.-Y., and Wang, H.: A new approach to separating the impacts of climate change and multiple human activities on water cycle processes based on a distributed hydrological model, *Journal of Hydrology*, 578, 124 096, 2019.
- Long, D., Longuevergne, L., and Scanlon, B. R.: Global analysis of approaches for deriving total water storage changes from GRACE satellites, *Water Resources Research*, 51, 2574–2594, <https://doi.org/10.1002/2015WR017096>. Received, 2015.
- Mahmood, R. and Jia, S.: Assessment of Impacts of Climate Change on the Water Resources of the Transboundary Jhelum River Basin of Pakistan and India, *Water*, 8, 246, <https://doi.org/10.3390/w8060246>, 2016.
- McCaig, M.: Contributions to storm quickflow in a small headwater catchment—the role of natural pipes and soil macropores, *Earth Surface Processes and Landforms*, 8, 239–252, 1983.
- Milly, P. C. D., Betancourt, J., Falkenmark, M., Hirsch, R. M., Kundzewicz, Z., Lettenmaier, D. P., Stouffer, R. J., Zbigniew, W., Lettenmaier, D. P., and Stouffer, R. J.: Stationarity Is Dead: Whither Water Management?, *Science*, 319, 573–574, <https://doi.org/10.1126/science.1151915>, 2008.
- Montanari, A. and Sideris, M. G.: Satellite Remote Sensing of Hydrological Change, *Global Change and Future Earth: The Geoscience Perspective*, 3, 57, 2018.
- Mu, Q., Zhao, M., and Running, S. W.: MODIS global terrestrial evapotranspiration (ET) product (NASA MOD16A2/A3), Algorithm Theoretical Basis Document, Collection, 5, 2013.
- Müller, M. and Thompson, S.: A value-based model selection approach for environmental random variables, *Water Resources Research*, 55, 270–283, 2019.
- Müller, M. F. and Levy, M. C.: Complementary vantage points: integrating hydrology and economics for sociohydrologic knowledge generation, *Water Resources Research*, 55, WR024 786, <https://doi.org/10.1029/2019WR024786>, 2019.
- Müller, M. F. and Thompson, S. E.: Bias adjustment of satellite rainfall data through stochastic modeling: Methods development and application to Nepal, *Advances in Water Resources*, 60, 121–134, 2013.
- Müller, M. F., Yoon, J., Gorelick, S. M., Avisse, N., and Tilmant, A.: Impact of the Syrian refugee crisis on land use and transboundary freshwater resources, *Proceedings of the national academy of sciences*, 113, 14 932–14 937, 2016.
- Nathan, R. J. and McMahon, T. A.: Evaluation of Automated Techniques for Baseflow and Recession Analysis, *Water Resources Research*, 26, 1465–1473, <https://doi.org/10.1029/WR026i007p01465>, 1990.
- Ning, T., Li, Z., Feng, Q., Liu, W., and Li, Z.: Comparison of the effectiveness of four Budyko-based methods in attributing long-term changes in actual evapotranspiration, *Scientific reports*, 8, 1–10, 2018.
- Penny, G., Srinivasan, V., Dronova, I., Lele, S., and Thompson, S.: Spatial characterization of long-term hydrological change in the Arkavathy watershed adjacent to Bangalore, India, *Hydrology and Earth System Sciences*, 22, 595–610, <https://doi.org/10.5194/hess-22-595-2018>, 2018.
- Penny, G., Mondal, M. S., Biswas, S., Bolster, D., Tank, J. L., and Müller, M. F.: Using Natural Experiments and Counterfactuals for Causal Assessment: River Salinity and the Ganges Water Agreement, *Water Resources Research*, 56, 1–15, <https://doi.org/10.1029/2019wr026166>, 2020a.



- Penny, G., Srinivasan, V., Apoorva, R., Jeremiah, K., Peschel, J., Young, S., and Thompson, S.: A process-based approach to attribution of historical streamflow decline in a data-scarce and human-dominated watershed, *Hydrological Processes*, 34, 1981–1995, <https://doi.org/10.1002/hyp.13707>, 2020b.
- Qiang, M., Hui-Jun, J., Bense, V. F., Dong-Liang, L., Marchenko, S. S., Harris, S. A., and Yong-Chao, L.: Impacts of degrading permafrost on streamflow in the source area of Yellow River on the Qinghai-Tibet Plateau, China, *Advances in Climate Change Research*, 10, 225–239, 2019.
- Railsback, L. B., Locke, W. W., and Johnson, J.: Comments and Reply on "Method of Multiple Working Hypotheses: A chimera", *Geology*, 18, 917–918, 1990.
- Rashid, I., Romshoo, S. A., and Abdullah, T.: The recent deglaciation of Kolahoi valley in Kashmir Himalaya, India in response to the changing climate, *Journal of Asian Earth Sciences*, 138, 38–50, <https://doi.org/10.1016/j.jseas.2017.02.002>, 2017.
- Romshoo, S. A.: Indus River Basin: Common Concerns and the Roadmap to Resolution, Tech. rep., Centre for Dialogue and Reconciliation, Srinagar, Kashmir, <http://www.slideshare.net/ShakilRomshoo/indus-river-basin-common-concerns-and>, 2012.
- Romshoo, S. A. and Rashid, I.: Assessing the impacts of changing land cover and climate on Hokersar wetland in Indian Himalayas, *Arabian Journal of Geosciences*, 7, 143–160, 2014.
- Romshoo, S. A., Dar, R. A., Rashid, I., Marazi, A., Ali, N., and Zaz, S. N.: Implications of Shrinking Cryosphere Under Changing Climate on the Streamflows in the Lidder Catchment in the Upper Indus Basin, India, *Arctic, Antarctic, and Alpine Research*, 47, 627–644, <https://doi.org/10.1657/AAAR0014-088>, 2015.
- Safeeq, M., Bart, R. R., Pelak, N. F., Singh, C. K., Dralle, D. N., Hartsough, P., and Wagenbrenner, J. W.: How realistic are water-balance closure assumptions? A demonstration from the southern Sierra Critical Zone Observatory and Kings River Experimental Watersheds, *Hydrol. Process.*, 2021.
- Savenije, H. H. G.: HESS Opinions "The art of hydrology", *Hydrology and Earth System Sciences*, 13, 157–161, <https://doi.org/10.5194/hess-13-157-2009>, 2009.
- Schaner, N., Voisin, N., Nijssen, B., and Lettenmaier, D. P.: The contribution of glacier melt to streamflow, *Environmental Research Letters*, 7, 034 029, 2012.
- Searcy, J. K. and Hardison, C. H.: Double-mass curves, 1541, US Government Printing Office, 1960.
- Sheffield, J., Wood, E. F., Verbist, K., Pan, M., Coccia, G., Beck, H., and Serrat-Capdevila, A.: Satellite Remote Sensing for Water Resources Management: Potential for Supporting Sustainable Development in Data-Poor Regions, *Water Resources Research*, 54, 9724–9758, <https://doi.org/10.1029/2017wr022437>, 2018.
- Shukla, A., Ali, I., Hasan, N., and Romshoo, S. A.: Dimensional changes in the Kolahoi glacier from 1857 to 2014, *Environmental monitoring and assessment*, 189, 1–18, 2017.
- Singh, P. and Kumar, N.: Impact assessment of climate change on the hydrological response of a snow and glacier melt runoff dominated Himalayan river, *Journal of Hydrology*, 193, 316–350, 1997.
- Sivapalan, M.: Pattern, process and function: elements of a unified theory of hydrology at the catchment scale, *Encyclopedia of hydrological sciences*, 2006.
- Sivapalan, M., Blöschl, G., Zhang, L., and Vertessy, R.: Downward approach to hydrological prediction, 2003.
- Smirnov, O., Zhang, M., Xiao, T., Orbell, J., Lobben, A., and Gordon, J.: The relative importance of climate change and population growth for exposure to future extreme droughts, *Climatic Change*, 138, 41–53, 2016.



- Srinivasan, V., Thompson, S., Madhyastha, K., Penny, G., Jeremiah, K., and Lele, S.: Why is the Arkavathy River drying? A multiple-hypothesis approach in a data-scarce region, *Hydrology and Earth System Sciences*, 19, 1905–1917, <https://doi.org/10.5194/hessd-12-25-2015>, 2015.
- Srinivasan, V., Konar, M., and Sivapalan, M.: A dynamic framework for water security, *Water Security*, 19, 4225, <https://doi.org/10.1016/j.wasec.2017.03.001>, 2017.
- 660 Strahler, A., Moody, A., Lambin, E., Huete, A., Justice, C., Muller, J., Running, S., Salomonson, V., Vanderbilt, V., and Wan, Z.: MODIS Land Cover Product: Algorithm Theoretical Basis Document (ATBD), Version 5.0, 1999.
- Thompson, S. E., Sivapalan, M., Harman, C. J., Srinivasan, V., Hipsey, M. R., Reed, P., Montanari, A., and Blöschl, G.: Developing predictive insight into changing water systems: use-inspired hydrologic science for the Anthropocene, *Hydrology and Earth System Sciences*, 17, 5013–5039, <https://doi.org/10.5194/hess-17-5013-2013>, 2013.
- 665 Tomer, M. D. and Schilling, K. E.: A simple approach to distinguish land-use and climate-change effects on watershed hydrology, *Journal of hydrology*, 376, 24–33, 2009.
- Valentín, J. M. P. and Müller, M. F.: Impact of Hurricane Maria on beach erosion in Puerto Rico: Remote sensing and causal inference, *Geophysical Research Letters*, 47, 2020.
- 670 Vermote, E.: MOD09A1 MODIS/terra surface reflectance 8-day L3 global 500m SIN grid V006, NASA EOSDIS Land Processes DAAC, 10, 2015.
- Viglione, A., Merz, B., Viet Dung, N., Parajka, J., Nester, T., and Blöschl, G.: Attribution of regional flood changes based on scaling fingerprints, *Water resources research*, 52, 5322–5340, 2016.
- Vörösmarty, C., Lettenmaier, D., Levêque, C., Meybeck, M., Pahl-Wostl, C., Alcamo, J., Cosgrove, W., Grassl, H., Hoff, H., Kabat, P., Lansigan, F., Lawford, R., and Naiman, R.: Human transforming the Global Water System, *Eos*, 85, 509–520, <https://doi.org/10.1029/2004EO480001>, 2004.
- 675 Wetlands International South Asia: Comprehensive Management Action Plan for Wular Lake, Tech. rep., Prepared for Department of Wildlife Protection Govt. of Jammu & Kashmir, <http://docplayer.net/37017787-Final-report-comprehensive-management-action-plan-for-wular-lake-kashmir-prepared-for-the-by.html>, 2007.
- 680 Wine, M. L. and Davison, J. H.: Untangling global change impacts on hydrological processes: Resisting climatization, *Hydrological Processes*, <https://doi.org/10.1002/hyp.13483>, 2019.
- Xu, H.: Modification of normalised difference water index (NDWI) to enhance open water features in remotely sensed imagery, *International journal of remote sensing*, 27, 3025–3033, 2006.
- Zaz, S. N., Romshoo, S. A., Krishnamoorthy, R. T., and Viswanadhapalli, Y.: Analyses of temperature and precipitation in the Indian Jammu and Kashmir region for the 1980–2016 period: implications for remote influence and extreme events, *Atmospheric Chemistry and Physics*, 19, 15–37, 2019.
- 685 Zhang, Z., Li, M., Si, B., and Feng, H.: Deep rooted apple trees decrease groundwater recharge in the highland region of the Loess Plateau, China, *Science of the Total Environment*, 622, 584–593, 2018.
- Zhao, S., Hu, H., Harman, C. J., Tian, F., Tie, Q., Liu, Y., and Peng, Z.: Understanding of storm runoff generation in a weathered, fractured granitoid headwater catchment in northern China, *Water*, 11, 1–22, <https://doi.org/10.3390/w11010123>, 2019.
- 690